

# Search for a lighter Higgs boson in the Next-to-Minimal Supersymmetric Standard Model<sup>\*</sup>

Jun-Quan Tao<sup>1,1)</sup> M. Aamir Shahzad<sup>1,2</sup> Si-Jing Zhang<sup>1,2,3</sup> Chu Wang<sup>1,2</sup>  
 Yu-Qiao Shen<sup>1,4</sup> Guo-Ming Chen<sup>1</sup> He-Sheng Chen<sup>1</sup> S. Gascon-Shotkin<sup>3</sup>  
 M. Lethuillier<sup>3</sup> L. Finco<sup>3</sup> C. Camen<sup>3</sup>

<sup>1</sup> Institute of High Energy Physics, Chinese Academy of Sciences, Beijing 100049, China

<sup>2</sup> University of Chinese Academy of Sciences, Beijing 100049, China

<sup>3</sup> Institut de Physique Nucléaire de Lyon, Université de Lyon,  
 Université Claude Bernard Lyon 1, CNRS-IN2P3, Villeurbanne 69622, France

<sup>4</sup> Changzhou Institute of Technology, Changzhou 213032, China

**Abstract:** Following the discovery of the Higgs boson with a mass of approximately 125 GeV at the LHC, many studies have been performed from both the theoretical and experimental viewpoints to search for a new Higgs Boson that is lighter than 125 GeV. We explore the possibility of constraining a lighter neutral scalar Higgs boson  $h_1$  and a lighter pseudo-scalar Higgs boson  $a_1$  in the Next-to-Minimal Supersymmetric Standard Model by restricting the next-to-lightest scalar Higgs boson  $h_2$  to be the one observed at the LHC after applying the phenomenological constraints and those from experimental measurements. Such lighter particles are not yet completely excluded by the latest results of the search for a lighter Higgs boson in the diphoton decay channel from LHC data. Our results show that some new constraints on the Next-to-Minimal Supersymmetric Standard Model could be obtained for a lighter scalar Higgs boson at the LHC if such a search is performed by experimental collaborations and more data. The potentials of discovery for other interesting decay channels of such a lighter neutral scalar or pseudo-scalar particle are also discussed.

**Keywords:** Next-to-Minimal Supersymmetric Standard Model, lighter Higgs boson, discovery potentials

**PACS:** 11.30.Pb, 14.80.Cp **DOI:** 10.1088/1674-1137/42/10/103107

## 1 Introduction

The Standard Model (SM) of particle physics has been highly successful in explaining high-energy experimental results. A Higgs boson with a mass of approximately 125 GeV was observed at the LHC with properties consistent with the Higgs boson predicted by the SM [1–4]. However, the observed signal strength of the Higgs boson is somewhat biased against the SM prediction within 1 or 2 times of the experimental uncertainty in each final state. Many important questions dealing with the nature and origin of the Higgs boson observed at the LHC remain unanswered. The Higgs boson can be embedded in some models beyond the Standard Model (BSM), such as supersymmetric models, which can eas-

ily accommodate the discovered Higgs boson and address the deficiencies of the Standard Model.

Supersymmetry (SUSY) [5–8] is one theoretical possibility for BSM physics. It introduces a symmetry between fermions and bosons. The most common framework and minimal realization of SUSY is the Minimal Supersymmetric Standard Model (MSSM) [9–11], which keeps limit the number of new fields and couplings to the minimum. In the MSSM, the Higgs sector contains two Higgs doublets, which leads to a spectrum including two CP-even, one CP-odd, and two charged Higgs bosons. The Lagrangian of the MSSM contains a supersymmetric mass term, namely the  $\mu$ -term. This mass term is invariant under supersymmetry, and therefore it seems unrelated to the electroweak scale, although it is

Received 31 May 2018, Published online 3 September 2018

<sup>\*</sup> Supported by National Natural Science Foundation of China (11505208, 11661141007, 11705016, 11875275), China Ministry of Science and Technology (2018YFA0403901) and partially by the France China Particle Physics Laboratory (FCPPL) and CAS Center for Excellence in Particle Physics (CCEPP)

1) E-mail: taojq@mail.ihep.ac.cn



Content from this work may be used under the terms of the Creative Commons Attribution 3.0 licence. Any further distribution of this work must maintain attribution to the author(s) and the title of the work, journal citation and DOI. Article funded by SCOAP<sup>3</sup> and published under licence by Chinese Physical Society and the Institute of High Energy Physics of the Chinese Academy of Sciences and the Institute of Modern Physics of the Chinese Academy of Sciences and IOP Publishing Ltd

phenomenologically required to be in this scale. This leads to the well-known “ $\mu$  problem” [12, 13] in the MSSM. In addition, the MSSM suffers from another serious flaw, namely the little hierarchy problem [14, 15]. The simplest solution is the so-called Next-to-Minimal Supersymmetric Standard Model (NMSSM), which introduces a new gauge singlet superfield that only couples to the Higgs sector in a similar manner to the Yukawa coupling, and can generate a  $\mu$  parameter dynamically of the order of the SUSY breaking scale, solving the “ $\mu$  problem” and the little hierarchy problem without requiring much fine-tuning [16–23]. Meanwhile, this new singlet adds additional degrees of freedom to the NMSSM particle spectrum. In the CP conserving case, which is assumed in this paper, the seven observable states in the Higgs sector can be classified into three CP-even Higgs bosons  $h_i$  ( $i = 1, 2, 3$ ), two CP-odd Higgs bosons  $a_j$  ( $j = 1, 2$ ), and two charged Higgs bosons  $h^\pm$ .

The extended parameter space of the NMSSM gives rise to a rich and interesting phenomenology. The lightest CP-even Higgs bosons ( $h_1$ ) with a mass range down to approximately 80 GeV, assuming the next-to-lightest CP-even Higgs boson  $h_2$  as the new particle observed with a mass of  $\sim 125$  GeV, was studied with the diphoton ( $\gamma\gamma$ ) final state in [24]. A Higgs decaying into  $\gamma\gamma$  is one of the two most promising channels for Higgs discovery at the LHC. The discovery prospects for a light scalar in the NMSSM [25] and Two-Higgs Doublet Models (2HDM) [26] have been considered, and comparisons with the CMS low mass diphoton analysis results at  $\sqrt{s} = 8$  TeV [27] have been performed. Recently, the CMS collaboration updated the results of the search for low mass Higgs bosons in the diphoton channel with the full 2016 data set at  $\sqrt{s} = 13$  TeV [28]. No significant excess has been observed by the CMS collaboration in the mass range of 70 GeV to 110 GeV. The observed upper bounds on the corresponding signal rate may help to place new constraints on the Next-to-Minimal Supersymmetric Standard Model.

In this paper, we explore the possibility of constraining a lighter neutral scalar Higgs boson  $h_1$  and a lighter pseudo-scalar Higgs boson  $a_1$  in the NMSSM by restricting the next-to-lightest scalar Higgs boson  $h_2$  to be the observed 125 GeV state, by comparing the lighter particles in the NMSSM with the latest CMS results with the full 2016 data set at  $\sqrt{s} = 13$  TeV, after the constraints from the experimental measurements and other sources have been imposed. The structure of this paper is as follows. In Section 2, we briefly introduce the Higgs sector of the NMSSM, the details of different constraints, and the chosen parameter ranges. Section 3 presents the results of the study for the lighter scalar Higgs boson  $a_1$ . Section 4 is dedicated to the study of the case in which the lighter resonance is the pseudo-scalar particle  $a_1$ . Finally, the conclusions are presented in Section 5.

## 2 NMSSM and constraints on the NMSSM

### 2.1 Description of NMSSM

The general NMSSM is a supersymmetric extension of the Standard Model that includes two Higgs superfields  $\hat{H}_u$  and  $\hat{H}_d$  and an additional gauge singlet chiral superfield  $\hat{S}$ . In this paper, we consider the NMSSM with a scale invariant superpotential  $W_{\text{NMSSM}}$  and the corresponding soft SUSY-breaking masses and couplings  $L_{\text{soft}}$ , both of which are limited to the R-parity and CP-conserving case. The superpotential  $W_{\text{NMSSM}}$ , depending on the Higgs superfields  $\hat{H}_u$  and  $\hat{H}_d$  and  $\hat{S}$ , can be expressed as [16]

$$W_{\text{NMSSM}} = h_u \hat{Q} \cdot \hat{H}_u \hat{U}_R^c + h_d \hat{H}_d \cdot \hat{Q} \hat{D}_R^c + h_e \hat{H}_d \cdot \hat{L} \hat{E}_R^c + \lambda \hat{S} \hat{H}_u \cdot \hat{H}_d + \frac{1}{3} \kappa \hat{S}^3. \quad (1)$$

In above formula, the first three terms on the right-hand side represent the Yukawa couplings of the quark and lepton superfields. The fourth term indicates that the  $\mu$ -term  $\mu \hat{H}_u \hat{H}_d$  of the MSSM superpotential is replaced by  $\lambda \hat{S} \hat{H}_u \hat{H}_d$ . The last term, which is cubic in the singlet superfield  $\hat{S}$ , is introduced to avoid the appearance of a Peccei-Quinn axion, which is tightly constrained by cosmological observations [16]. The corresponding soft SUSY-breaking masses and couplings are given in the SLHA2 [29] conventions by the following equation [16]:

$$\begin{aligned} -L_{\text{soft}} = & m_{H_u}^2 |H_u|^2 + m_{H_d}^2 |H_d|^2 + m_S^2 |S|^2 + m_Q^2 |Q|^2 \\ & + m_U^2 |U_R|^2 + m_D^2 |D_R|^2 + m_L^2 |L|^2 + m_E^2 |E_R|^2 \\ & + h_u A_u Q \cdot H_u U_R^c - h_d A_d Q \cdot H_d D_R^c - h_e A_e L \cdot H_d E_R^c \\ & + \lambda A_\lambda H_u \cdot H_d S + \frac{1}{3} \kappa A_\kappa S^3 + \text{h.c.} \end{aligned} \quad (2)$$

In the above Eq. 1 and Eq. 2, it is clear that the non-zero vacuum expectation value  $s$  of the singlet  $\hat{S}$  of the order of the weak or SUSY-breaking scale gives rise to an effective  $\mu$ -term with

$$\mu_{\text{eff}} = \lambda s. \quad (3)$$

Here,  $\lambda$  is dimensionless, hence the “ $\mu$  problem” of the MSSM is solved. Meanwhile, the three SUSY-breaking mass-squared terms for  $H_u$ ,  $H_d$ , and  $S$  in  $L_{\text{soft}}$  can be expressed as functions of their VEVs (vacuum expectation values) through the three minimization conditions of the scalar potential. Therefore, the Higgs sector of the NMSSM is described by the following six parameters:

$$\lambda, \kappa, A_\lambda, A_\kappa, \tan\beta = \frac{\langle H_u \rangle}{\langle H_d \rangle}, \mu_{\text{eff}} = \lambda \langle S \rangle, \quad (4)$$

in which each pair of brackets denotes the VEV of the respective superfield inside them. Besides these six

parameters of the Higgs sector, the squark and slepton soft SUSY-breaking masses and the trilinear couplings, as well as the gaugino soft SUSY-breaking masses, also must be specified, as described in the following section, in order to describe the model completely.

## 2.2 Constraints on the NMSSM and its parameters

The program package NMSSMTools (version 5.2.0) [30] is employed in this study to calculate the SUSY particles, the spectrums of the NMSSM Higgs bosons, their decaying branching ratios (BR), and the reduced couplings of the NMSSM Higgs bosons to other particles. NMSSMTools contains four subpackages, NMHDECAY, NMSDECAY, NMSPEC, and NMGMSB. The FORTRAN code NMHDECAY provides the masses, decay widths, branching ratios and reduced couplings to other particles, for Higgs bosons that will be used in this paper. In this paper, we consider the four Higgs production modes of gluon-gluon fusion through a heavy quark loop (ggh), the vector boson fusion process (vbf), the associate production of Higgs with a vector boson (vh), and the associated production of a Higgs with a pair of top quarks (tth). The cross sections for different production modes of each NMSSM Higgs boson are obtained from the linear interpolation of the 5 GeV per step cross section values taken from the handbook of the LHC Higgs Cross Section Working Group [31] for a SM-like BSM Higgs boson, and multiplied by the reduced couplings of each NMSSM Higgs boson to gluons  $\kappa_g^2$ , gauge bosons  $\kappa_V^2$ , and fermions  $\kappa_f^2$ , which are given by the output of NMSSMTools. The NMSSMTools package applies all phenomenological constraints, including the absence of Landau singularities below the GUT scale and the constraints from flavor physics, dark matter relic density  $\Omega h^2$ , anomalous magnetic moment of the muon ( $g-2$ ), Higgs searches in various channels, and direct searches for SUSY particles at LEP, Tevatron, and

LHC, with the details described in [30].

The six NMSSM specific parameters described above are varied in the following ranges:

$$\begin{aligned} 0.55 < \lambda < 0.75, \quad 0.05 < \kappa < 0.3, \quad 3 < \tan\beta < 6, \\ 150 \text{ GeV} < \mu_{\text{eff}} < 350 \text{ GeV}, \\ -500 \text{ GeV} < A_\kappa < 0 \text{ GeV}, \\ 500 \text{ GeV} < A_\lambda < 1600 \text{ GeV}. \end{aligned} \quad (5)$$

To choose values of  $\lambda$  and  $\kappa$  that are sufficiently large but small enough to avoid a Landau pole below the GUT scale and low values for  $\tan\beta$  that naturally keep the amount of fine-tuning as low as possible is suitable for this study. We found that wider ranges of the trilinear couplings  $A_\kappa$ ,  $A_\lambda$ , and  $\mu_{\text{eff}}$  have practically no impact on our results.

The soft SUSY-breaking mass terms for the squark ( $M_U$ ,  $M_D$ , and  $M_Q$ ) and sleptons ( $M_L$  and  $M_E$ ), the soft SUSY-breaking trilinear couplings ( $A_D$ ,  $A_E$ , and  $A_U$ ), the gluino mass ( $M_3$ ), and the other soft SUSY-breaking gaugino masses ( $M_1$  and  $M_2$ ) have been set as

$$\begin{aligned} M_Q = M_U = M_D = 1000 \text{ GeV}, \\ M_L = M_E = 300 \text{ GeV}, \\ A_D = A_E = A_U = 1000 \text{ GeV}, \\ 100 \text{ GeV} < M_1 < 150 \text{ GeV}, \\ 150 \text{ GeV} < M_2 < 250 \text{ GeV}, \\ 1000 \text{ GeV} < M_3 < 2000 \text{ GeV}. \end{aligned} \quad (6)$$

Using the NMSSMTools package and the general NMSSM model, we have performed random scans with about 10 billion points in the specific parameter space described above. For each point in the parameter space satisfying the phenomenological constraints, we require that an SM-like Higgs state, the next-to-lightest scalar Higgs boson  $h_2$  in NMSSM, must be within the allowed theoretical uncertainty of 3 GeV around the measured mass 125.1 GeV at the LHC using the whole Run1

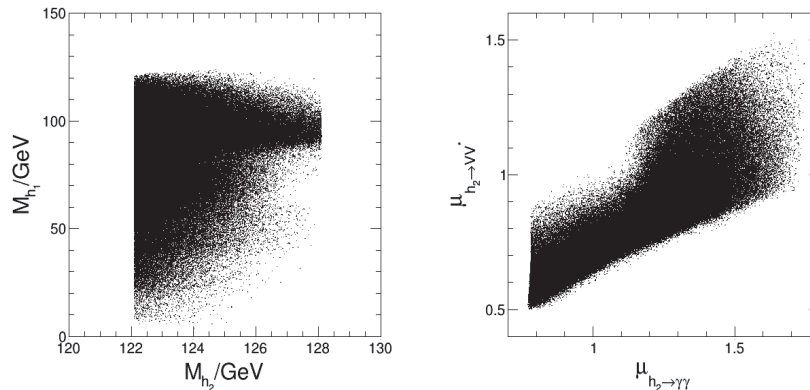


Fig. 1. Mass spectrum of the two lightest scalar Higgs bosons  $h_1$  and  $h_2$  (left panel), and the signal strengths of  $h_2 \rightarrow \gamma\gamma$  versus the signal strengths of  $h_2 \rightarrow VV^*$  (right panel), from the NMSSM scans with the constraints.

data [32] ( $125.1 \pm 3$  GeV) and couplings of  $h_2$  to gauge bosons and fermions in the  $3\sigma$  ranges of the best-fit values given in [33, 34]. With these constraints, around 1.40 million points remain. Fig. 1 shows the mass distributions of the two lightest scalar Higgs bosons  $h_1$  and  $h_2$ , and the signal strengths of  $h_2 \rightarrow \gamma\gamma$  versus the signal strengths of  $h_2 \rightarrow VV^*$  ( $VV^* = ZZ/W^+W^-$ ), with the signal strength defined as the relative ratio of the cross section time branching ratio of the Higgs boson from each NMSSM point to the SM-like BSM predicted value from the handbook of the LHC Higgs Cross Section Working Group [31].

With the full 2016 data set at  $\sqrt{s} = 13$  TeV, the CMS collaboration have updated the results for searching for a light resonance decaying into two photons in the mass range from 70 GeV to 110 GeV [28]. To compare with the experimental sensitivity and to explore the discovery potentials for other interesting decay channels, the masses of the lightest scalar Higgs boson  $h_1$  and the lightest pseudo-scalar Higgs boson  $a_1$  are constrained in the range from 60 GeV to 120 GeV in the following sections.

### 3 Results for a lighter scalar Higgs boson

In this section, we will explore the possibility that the signal may be given by the lightest scalar Higgs boson  $h_1$  in the NMSSM. We perform a detailed comparison with the sensitivity of the CMS search at 13 TeV. About 1.25 million points are selected from the random scans passing the phenomenological constraints, the mass and signal strength constraints on  $h_2$ , and the mass constraint on  $h_1$  with a mass range from 60 GeV to 120 GeV.

The left panel of Fig. 2 shows the signal strengths of  $h_1$  decaying into a diphoton  $\mu_{h_1 \rightarrow \gamma\gamma}$  plotted against the mass of the Higgs boson  $h_1$  ( $M_{h_1}$ ). It can be seen that a

sizable enhancement over the SM-like Higgs rate is possible for the Higgs boson  $h_1$ , with the largest strength  $\sim 2.2$  occurring at an  $h_1$  mass of  $\sim 85$  GeV. We note that for the mass ranges  $M_{h_1} < \sim 80$  GeV and  $M_{h_1} > \sim 110$  GeV, the allowed signal strengths  $\mu_{h_1 \rightarrow \gamma\gamma}$  are considerably lower than 1. In particular, for  $M_{h_1} < \sim 75$  GeV the signal strengths are below  $\sim 0.2$ . The production rates in femtobarns ( $fb$ ) of  $h_1$  decaying into  $\gamma\gamma$  versus  $M_{h_1}$  are also plotted for the combined ggh and tth production mode ( $(\sigma \times BR)_{h_1 \rightarrow \gamma\gamma}^{ggh+tth}$ ) in the middle panel and for the combined vbf and vh production mode ( $(\sigma \times BR)_{h_1 \rightarrow \gamma\gamma}^{vbf+vh}$ ) in the right panel of Fig. 2, superimposed on the public observed exclusion limits of the CMS collaboration with the full 2016 data set at  $\sqrt{s} = 13$  TeV [28] shown by the red line. These comparisons show that there is no sensitivity in the vbf+vh production mode, but many points are above the CMS observed upper limit in the ggh+tth production mode for a light Higgs boson with mass  $M_{h_1} > \sim 80$  GeV. For the vbf+vh production mode, it is possible to obtain points above the CMS observed upper limit in the near future with more proton-proton collision data accumulated at the LHC.

As the points above the observed CMS upper limit are excluded at the 95% confidence level, we can expect to exclude some NMSSM region in the parameter space thanks to this analysis. To illustrate this point, in Fig. 3 we compare several sensitivity parameters for two different cases. The top three figures show all the selected 1.25 million points in the 2D planes of  $\tan\beta$  vs  $\lambda$ ,  $\lambda$  vs  $\kappa$ , and  $\mu_{\text{eff}}$  vs  $\kappa$ . The bottom panel shows the corresponding figures for the points with  $(\sigma \times BR)_{h_1 \rightarrow \gamma\gamma}$  above the CMS observed upper limit, and consequently excluded by the experiment in the mass range from 70 GeV to 110 GeV. The parameter ranges of the excluded points overlap with the rest points that are not excluded by the experiment. Therefore, we cannot conclude that the

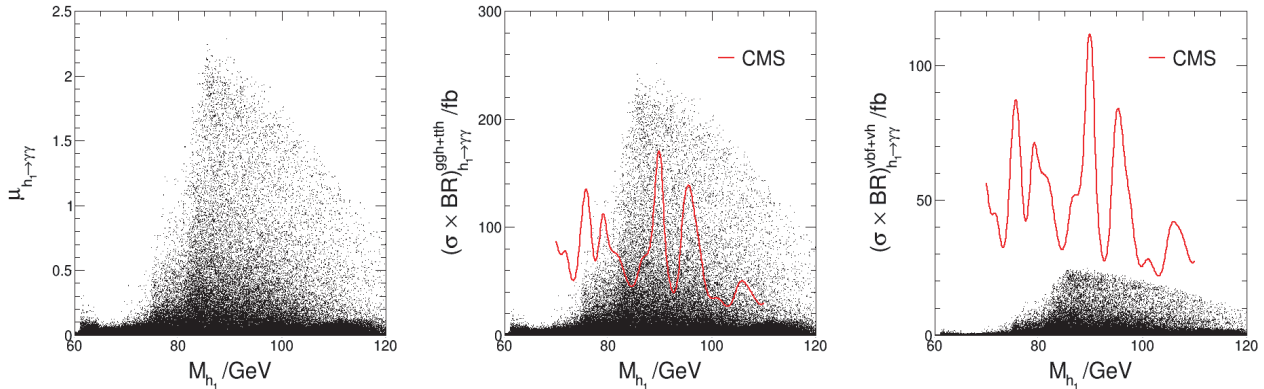


Fig. 2. (color online) Signal strengths of  $h_1$  decaying into the diphoton ( $\mu_{h_1 \rightarrow \gamma\gamma}$ ) versus the mass of  $h_1$  (left panel) and the signal rates as functions of the  $h_1$  mass generated in the general NMSSM superimposed on the observed results of the CMS 13 TeV low-mass diphoton analysis [28] in the combined ggh and tth production mode  $(\sigma \times BR)_{h_1 \rightarrow \gamma\gamma}^{ggh+tth}$  (middle panel) and in the combined vbf and vh production mode  $(\sigma \times BR)_{h_1 \rightarrow \gamma\gamma}^{vbf+vh}$  (right panel).

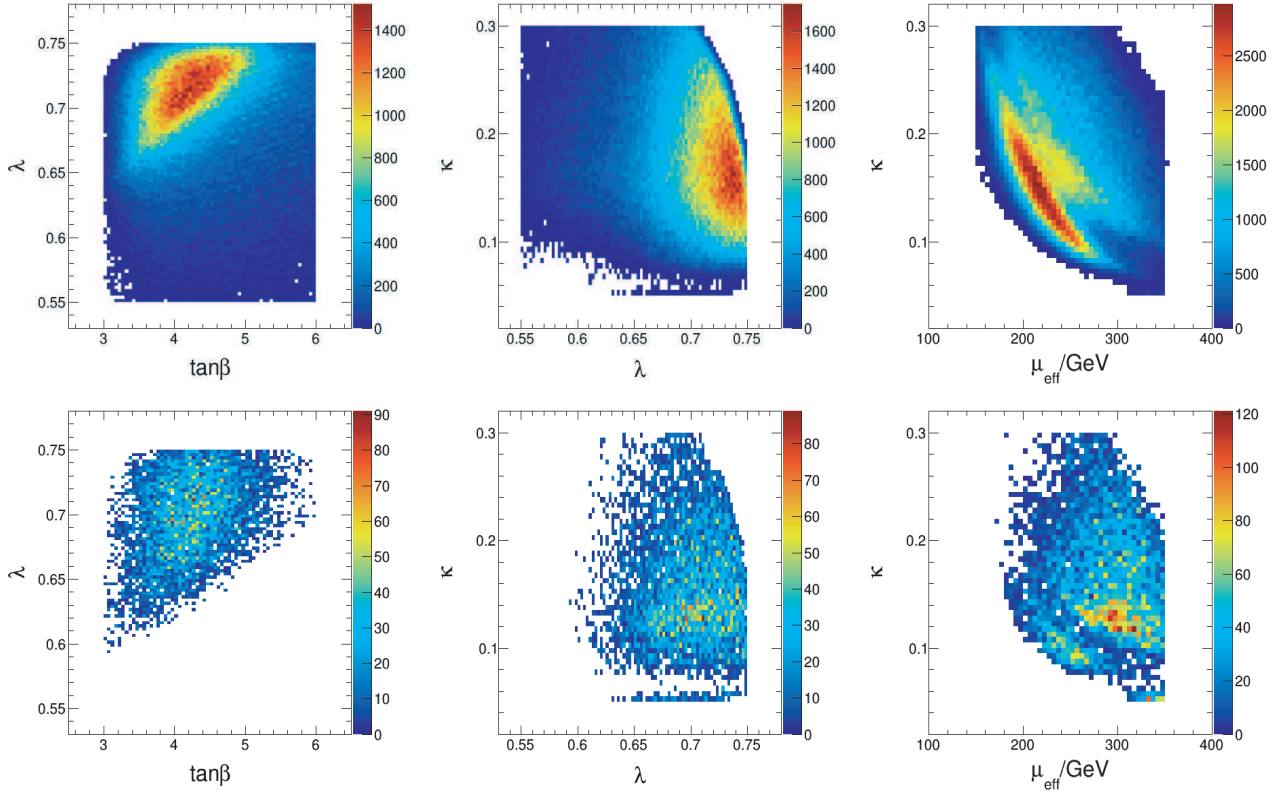


Fig. 3. (color online) Two-dimensional scatter plots of the input parameters  $\tan\beta$  vs  $\lambda$ ,  $\lambda$  vs  $\kappa$ , and  $\mu_{\text{eff}}$  vs  $\kappa$  for all selected points passing the phenomenological constraints, the mass and signal strength constraints on  $h_2$ , and the mass constraint on  $h_1$  with a mass range from 60 GeV to 120 GeV are shown in the top panels. The corresponding two-dimensional scatter plots of the input parameters for the selected points further excluded by the observed upper limits of the CMS 13 TeV low-mass diphoton analysis with a mass range from 70 GeV to 110 GeV are shown in the bottom panels.

parameter ranges shown in the bottom three figures are excluded by the experiment. Nevertheless, it can be seen by comparing of the top and bottom figures that the points with higher  $\tan\beta$  but lower  $\lambda$  from the bottom-left panel, with lower  $\lambda$  ( $< 0.6$ ) from the bottom-middle panel, or with lower  $\mu_{\text{eff}}$  ( $< 180$  GeV) from the bottom-right panel are not sufficiently sensitive to larger production rates to be excluded by the experiment. The excluded points populate the parameter space with  $\tan\beta$  around 4,  $\lambda$  around 7,  $\kappa$  around 0.13, and  $\mu_{\text{eff}}$  around 300 GeV.

In addition, we also checked the production rates of other interesting decay channels, including  $b\bar{b}$ ,  $\tau^+\tau^-$ ,  $W^+W^-$ ,  $ZZ$ ,  $Z\gamma$ , and  $\mu^+\mu^-$ , to investigate the discovery potentials of  $h_1$  in these channels. Fig. 4 shows the production rates in picobarns (pb) for  $h_1$  decaying into  $b\bar{b}$ ,  $\tau^+\tau^-$ ,  $W^+W^-$ ,  $ZZ$ ,  $Z\gamma$ , and  $\mu^+\mu^-$ , as functions of its mass  $M_{h_1}$ . The  $h_1 \rightarrow b\bar{b}$ ,  $h_1 \rightarrow \tau^+\tau^-$ , and  $h_1 \rightarrow \mu^+\mu^-$  decay have tight correlations on the branching ratios, although with different values. Therefore, the shapes of their production rates as functions of  $M_{h_1}$  are similar. In addition, the similar shapes of production rates of

$h_1 \rightarrow W^+W^-$ ,  $h_1 \rightarrow ZZ$  and  $h_1 \rightarrow Z\gamma$  are a result of the tight correlations on the branching ratios. Among these decay channels, the signal rate of  $h_1 \rightarrow b\bar{b}$  is reasonably large, as the rates can reach up to 18 pb with  $M_{h_1}$  at around 95 GeV. For the  $h_1 \rightarrow W^+W^-$ ,  $h_1 \rightarrow ZZ$ , and  $h_1 \rightarrow Z\gamma$  channels, the signal rates decrease with decreasing  $M_{h_1}$ . For the  $b\bar{b}$  and  $\tau^+\tau^-$  final states in the investigated mass range, the signal rates are sufficiently large that it is very possible to detect  $h_1$  by experiments at the LHC via these two channels.

#### 4 Results for a lighter pseudo-scalar Higgs boson

As the kinematic behavior of the two photons coming from the decay of a pseudo-scalar particle is very similar to that resulting from a scalar particle [35], we can directly apply the CMS study as in the scalar case to constrain a possible light pseudo-scalar. Because the mass of the heavier pseudo-scalar  $a_2$  from NMSSM scans is considerably larger than that of the Higgs observed at the LHC, we focus on the lightest pseudo-scalar  $a_1$  in the



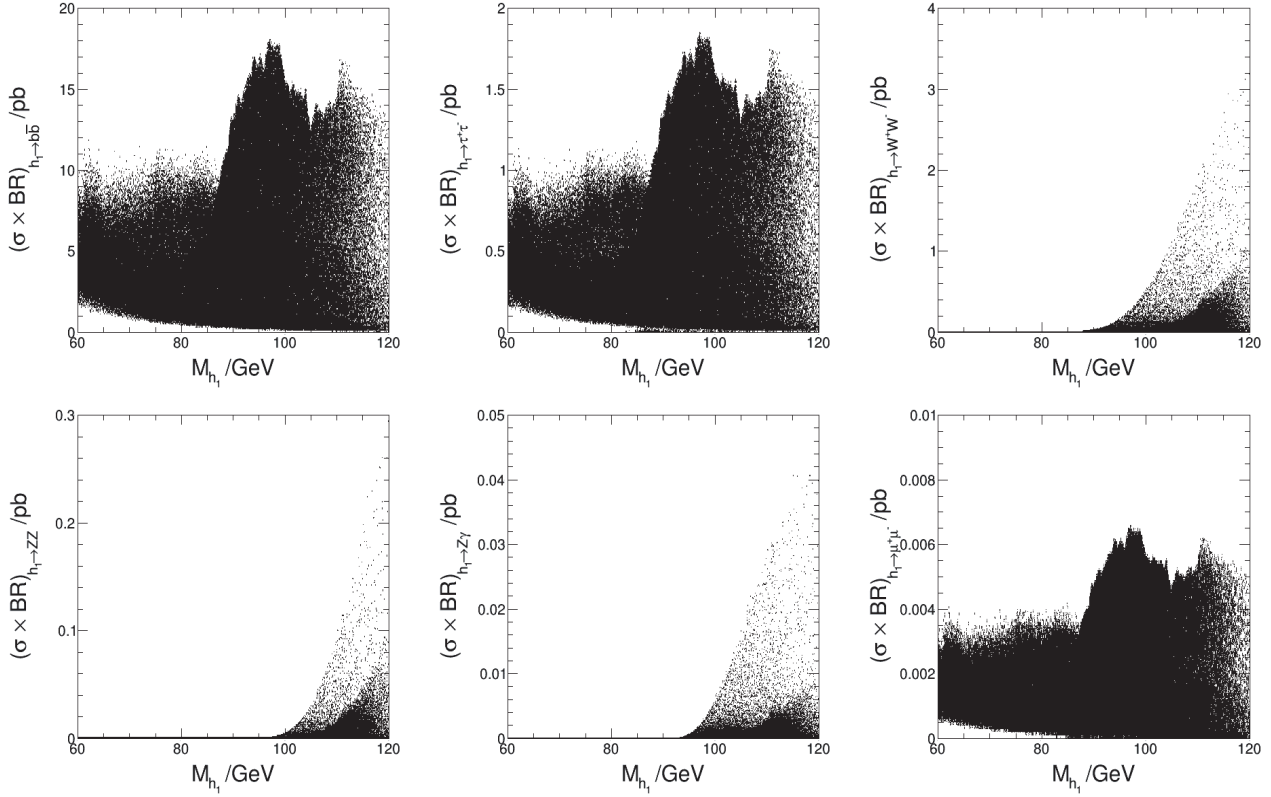


Fig. 4. Signal rates as functions of the  $h_1$  mass for other interesting decay channels:  $(\sigma \times BR)_{h_1 \rightarrow b\bar{b}}$  (top left),  $(\sigma \times BR)_{h_1 \rightarrow \tau^+\tau^-}^{ggh+tth}$  (top middle),  $(\sigma \times BR)_{h_1 \rightarrow W^+W^-}^{vbf+vh}$  (top right),  $(\sigma \times BR)_{h_1 \rightarrow ZZ}^{ggh+tth}$  (bottom left),  $(\sigma \times BR)_{h_1 \rightarrow Z\gamma}^{vbf+vh}$  (bottom middle), and  $(\sigma \times BR)_{h_1 \rightarrow \mu^+\mu^-}^{vbf+vh}$  (bottom right).

following. From the random scans after the phenomenological constraints and the mass and signal strength constraints on  $h_2$  have been imposed, the mass distributions of the lightest pseudo-scalar  $a_1$  versus the scalar Higgs bosons  $h_2$  are shown in the top left panel of Fig. 5. Then, about 187,000 points are selected after the constraint of  $a_1$  within the mass range from 60 GeV to 120 GeV has been imposed.

The lightest CP-odd Higgs boson  $a_1$  primarily decays to fermions, owing to the absence of tree-level couplings with gauge bosons. As shown in the top-right panel of Fig. 5, it decays dominantly to  $b\bar{b}$  with BR  $\sim 90\%$  for the low mass range. For  $a_1 \rightarrow \gamma\gamma$  with  $a_1$  in the mass range of 60 GeV to 120 GeV, the BR is less than  $7 \times 10^{-4}$  for all the selected points. As shown in the bottom left panel, the signal rates of  $a_1 \rightarrow \gamma\gamma$  for all the selected points in the combined ggh and tth production mode are lower than 0.3 fb, which is far below the CMS-observed upper limits, as the red line shows in the middle panel of Fig. 2. In addition, for the combined vbf and vh production mode the signal rates of  $a_1 \rightarrow \gamma\gamma$  with the points shown in the bottom right panel of Fig. 5 are also far below the CMS-observed upper limit on the production cross-section times the branching ratio, as the red line shows in the right panel of Fig. 2. Therefore, we conclude

that CMS had no sensitivity to a light pseudo-scalar in the diphoton final state with the data collected in the year 2016.

We have also checked the production rates for other interesting decay channels of  $a_1$ , to investigate the discovery potentials of  $a_1$  in these channels. Fig. 6 shows the production rates in femtobarns (fb) for  $a_1$  decaying into  $b\bar{b}$ ,  $\tau^+\tau^-$ ,  $W^+W^-$ ,  $ZZ$ ,  $Z\gamma$ , and  $\mu^+\mu^-$  as functions of its mass  $M_{a_1}$ . As expected,  $a_1 \rightarrow b\bar{b}$  is the dominant decay channel, with signal rates of up to about 3800 fb, and  $h_1 \rightarrow \tau^+\tau^-$  is the sub-dominant decay channel, with signal rates of up to about 300 fb. For the  $b\bar{b}$  decay of  $a_1$ , the cross section is sufficiently large to search for  $a_1$  at the LHC if the large backgrounds can be well suppressed. As for the top quark pair final states, it is also possible to detect a low-mass  $a_1$  in this channel. Considering the BRs of the cascade decays of  $W$  and  $Z$ , it will be difficult to search for  $a_1$  with the  $W^+W^-$  and  $ZZ$  channels with all the LHC Run2 data. It is also difficult to search for  $a_1$  with  $h_1 \rightarrow \mu^+\mu^-$ , owing to the small signal rates and the acceptance times the selection efficiency for the signal events, which is  $\sim 50\%$  for a 125 GeV SM Higgs boson [36, 37]. For the lower signal rates of  $Z\gamma$  decay, it is impossible to search for  $a_1$  in the  $Z\gamma$  channel for all LHC Run2 data.

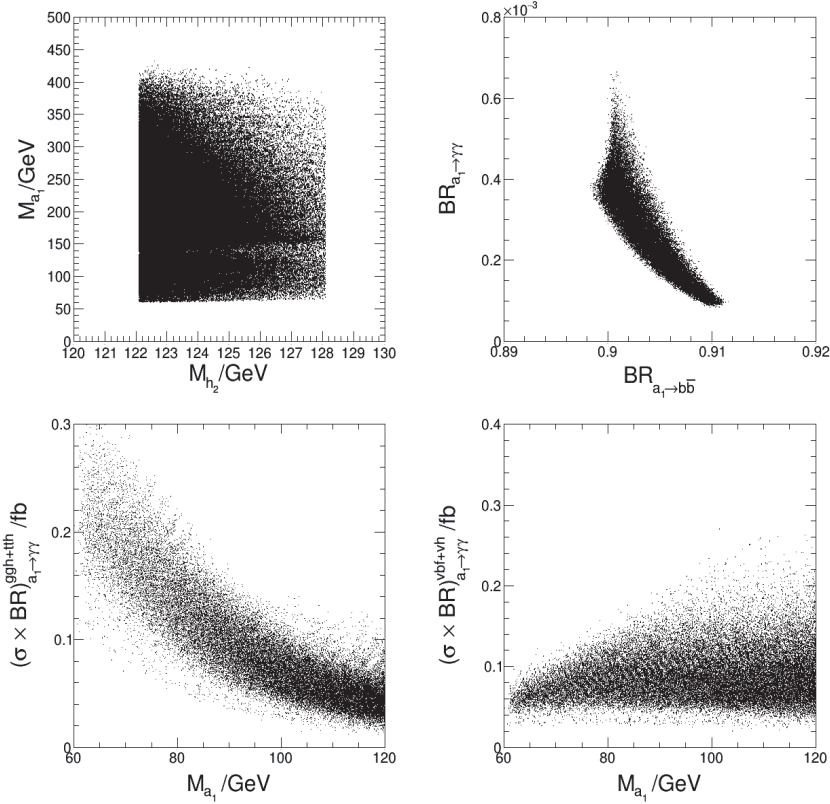


Fig. 5. Mass spectrum of the lightest pseudo-scalar Higgs bosons  $a_1$  versus  $h_2$  (top left panel) after the phenomenological constraints and constraints on  $h_2$  have been imposed, distributions of the branching ratios of  $a_1 \rightarrow b\bar{b}$  versus  $a_1 \rightarrow \gamma\gamma$  (top right) and the signal rates of  $a_1 \rightarrow \gamma\gamma$  versus the mass of  $a_1$  for different combined production modes with  $(\sigma \times BR)_{a_1 \rightarrow \gamma\gamma}^{ggh+tth}$  for ggh+tth (bottom left), and  $(\sigma \times BR)_{a_1 \rightarrow \gamma\gamma}^{vbf+vh}$  for vbf+vh (bottom right) after the further mass constraint on  $a_1$  has been imposed.

## 5 Conclusions

Following the discovery of the Higgs boson with a mass of approximately 125 GeV at the LHC, many studies from both the theoretical and experimental viewpoints have been performed to search for a new Higgs Boson that is lighter than 125 GeV. The search for such a lighter Higgs Boson represents one of the most important avenues for probing the possible structure of physics beyond the Standard Model. In this paper, we explored the possibility of constraining a lighter neutral scalar Higgs boson  $h_1$  and a lighter pseudo-scalar Higgs boson  $a_1$  in the Next-to-Minimal Supersymmetric Standard Model by restricting the next-to-lightest scalar Higgs boson  $h_2$  to be the LHC observed Higgs boson after the phenomenological constraints and constraints from experimental measurements have been imposed. Such a lighter particle is not yet completely excluded by the latest results of the search for a lighter Higgs boson with the

diphoton decay channel from the LHC data collected by the CMS detector at 13 TeV. For a lighter neutral scalar  $h_1$ , we can expect to exclude some NMSSM region in the parameter space. While the latest CMS results shows no sensitivity to a light pseudo-scalar in the diphoton final state, our results show that some new constraints on the Next-to-Minimal Supersymmetric Standard Model could be obtained at the LHC if such a search is performed by the experimental collaborations with additional data in the future. The discovery potentials for other interesting decay channels of such a lighter neutral scalar or pseudo-scalar particle have also been discussed. For the  $b\bar{b}$  and  $\tau^+\tau^-$  final states of both  $h_1$  and  $a_1$  in the investigated mass range, it is possible to detect such lighter particles by the experiments at the LHC.

*The authors would like to thank Ulrich Ellwanger and Cyril Hugonie for helpful discussions.*

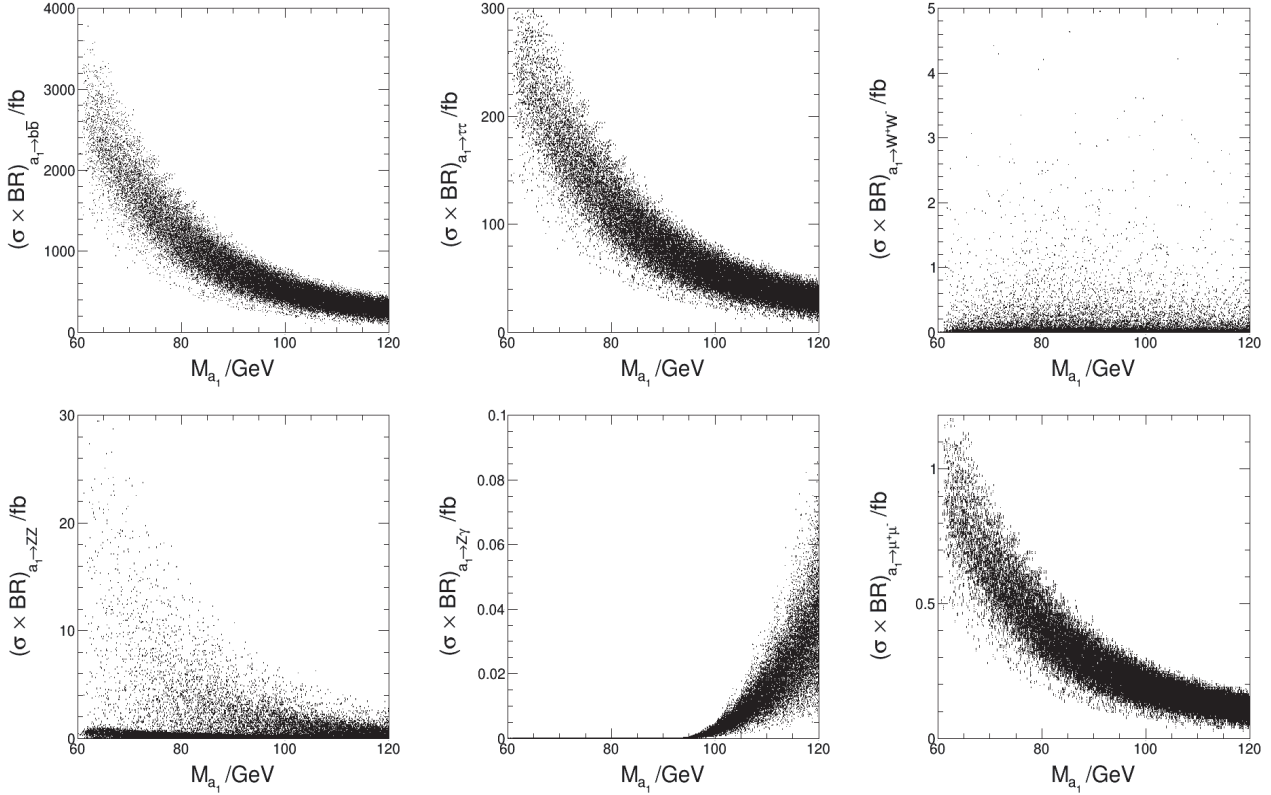


Fig. 6. Signal rates as functions of the  $a_1$  mass for other interesting decay channels:  $(\sigma \times BR)_{a_1 \rightarrow b\bar{b}}$  (top left),  $(\sigma \times BR)_{a_1 \rightarrow \tau^+\tau^-}$  (top middle),  $(\sigma \times BR)_{a_1 \rightarrow W^+W^-}$  (top right),  $(\sigma \times BR)_{a_1 \rightarrow ZZ}$  (bottom left),  $(\sigma \times BR)_{a_1 \rightarrow Z\gamma}$  (bottom right), and  $(\sigma \times BR)_{a_1 \rightarrow \mu^+\mu^-}$  (bottom right).

## References

- 1 G. Aad et al (ATLAS Collaboration), Phys. Lett. B, **716**: 1 (2012)
- 2 S. Chatrchyan et al (CMS Collaboration), Phys. Lett. B, **716**: 30 (2012)
- 3 G. Aad et al (ATLAS Collaboration), Phys. Lett. B, **726**: 88 (2013); Erratum: [Phys. Lett. B, **734**: 406 (2014)]
- 4 S. Chatrchyan et al (CMS Collaboration), JHEP, **1306**: 081 (2013)
- 5 P. Fayet, Phys. Lett. B, **64**: 159 (1976)
- 6 P. Fayet, Phys. Lett. B, **69**: 489 (1977)
- 7 G. R. Farrar and P. Fayet, Phys. Lett. B, **76**: 575 (1978)
- 8 G. F. Giudice, M. A. Luty, H. Murayama, and R. Rattazzi, JHEP, **9812**: 027 (1998)
- 9 H. P. Nilles, Phys. Rept., **110**: 1 (1984)
- 10 H. E. Haber and G. L. Kane, Phys. Rept., **117**: 75 (1985)
- 11 R. Barbieri, Riv. Nuovo Cim., **11N4**: 1 (1988)
- 12 J. E. Kim and H. P. Nilles, Phys. Lett. B, **138**: 150 (1984)
- 13 G. F. Giudice and A. Masiero, Phys. Lett. B, **206**: 480 (1988)
- 14 S. Weinberg, Phys. Lett. B, **82**: 387 (1979)
- 15 C. H. Llewellyn Smith and G. G. Ross, Phys. Lett. B, **105**: 38 (1981)
- 16 U. Ellwanger, C. Hugonie, and A. M. Teixeira, Phys. Rept., **496**: 1 (2010)
- 17 U. Ellwanger, JHEP, **1203**: 044 (2012)
- 18 J. F. Gunion, Y. Jiang, and S. Kraml, Phys. Rev. D, **86**: 071702 (2012)
- 19 S. F. King, M. Muhlleitner, and R. Nevzorov, Nucl. Phys. B, **860**: 207 (2012)
- 20 J. J. Cao, Z. X. Heng, J. M. Yang, Y. M. Zhang, and J. Y. Zhu, JHEP, **1203**: 086 (2012)
- 21 K. Agashe, Y. Cui, and R. Franceschini, JHEP, **1302**: 031 (2013)
- 22 K. Kowalska, S. Munir, L. Roszkowski, E. M. Sessolo, S. Trojanowski, and Y. L. S. Tsai, Phys. Rev. D, **87**: 115010 (2013)
- 23 T. Gherghetta, B. von Harling, A. D. Medina, and M. A. Schmidt, JHEP, **1302**: 032 (2013)
- 24 J. W. Fan, J. Q. Tao et al, Chin. Phys. C, **38**: 073101 (2014)
- 25 U. Ellwanger and M. Rodriguez-Vazquez, JHEP, **1602**: 096 (2016)
- 26 G. Cacciapaglia, A. Deandrea, S. Gascon-Shotkin, S. Le Corre, M. Lethuillier, and J. Tao, JHEP, **1612**: 068 (2016)
- 27 CMS Collaboration (CMS Collaboration), CMS-PAS-HIG-14-037
- 28 CMS Collaboration (CMS Collaboration), CMS-PAS-HIG-17-013
- 29 B. C. Allanach et al, Comput. Phys. Commun., **180**: 8 (2009)
- 30 <http://www.th.u-psud.fr/NMHDECAY/nmsmtools.html>
- 31 D. de Florian et al (LHC Higgs Cross Section Working Group)
- 32 G. Aad et al (ATLAS and CMS Collaborations), Phys. Rev. Lett., **114**: 191803 (2015)
- 33 G. Aad et al (ATLAS and CMS Collaborations), JHEP, **1608**: 045 (2016)
- 34 J. Bernon, B. Dumont, and S. Kraml, Phys. Rev. D, **90**: 071301 (2014)
- 35 P. Artoisenet et al, JHEP, **1311**: 043 (2013)
- 36 CMS Collaboration (CMS Collaboration), CMS-PAS-HIG-17-019
- 37 M. Aaboud et al (ATLAS Collaboration), Phys. Rev. Lett., **119**(5): 051802 (2017)